Estimating loss of life caused by dam breaches based on the simulation of floods routing and evacuation potential of population at risk

Ge, Wei; Jiao, Yutie; Wu, Meimei; Li, Zongkun; Wang, Te; Li, Wei; Zhang, Yadong; Gao, Weixing; van Gelder, Pieter

DOI
10.1016/j.jhydrol.2022.128059

Publication date
2022

Document Version
Final published version

Published in
Journal of Hydrology

Citation (APA)
Ge, W., Jiao, Y., Wu, M., Li, Z., Wang, T., Li, W., Zhang, Y., Gao, W., & van Gelder, P. (2022). Estimating loss of life caused by dam breaches based on the simulation of floods routing and evacuation potential of population at risk. *Journal of Hydrology*, *612*, 11. Article 128059. https://doi.org/10.1016/j.jhydrol.2022.128059

Journal of Hydrology 612 (2022) 128059

Contents lists available at ScienceDirect

Journal of Hydrology

journal homepage: www.elsevier.com/locate/jhydrol

Research papers

Estimating loss of life caused by dam breaches based on the simulation of floods routing and evacuation potential of population at risk

Wei Ge [a], Yutie Jiao [a], Meimei Wu [b,*], Zongkun Li [a], Te Wang [a], Wei Li [c], Yadong Zhang [a], Weixing Gao [d], Pieter van Gelder [e]

[a] School of Water Conservancy Engineering, Zhengzhou University, Zhengzhou 450001, PR China
[b] College of Civil Engineering and Architecture, Henan University of Technology, Zhengzhou 450001, PR China
[c] School of Railway Engineering, Zhengzhou Railway Vocational and Technical College, Zhengzhou 450001, PR China
[d] School of Political Science and Public Administration, Zhengzhou University, Zhengzhou 450001, PR China
[e] Safety and Security Science Group (S3G), Faculty of Technology, Policy and Management, Delft University of Technology, Delft 2628 BX, the Netherlands

ARTICLE INFO

This manuscript was handled by Nandita Basu, Editor-in-Chief, with the assistance of Julianne Quinn, Associate Editor

Keywords:
Dam breach
Loss of life
Disaster-causing mechanism
Evacuation potential
Emergency plan

ABSTRACT

Dam breaches often have catastrophic consequences in downstream areas. Hydrodynamic factors and the evacuation potential of the population at risk (*PAR*) have significant impacts on the loss of life (*LOL*) caused by dam breaches. However, the existing comprehensive evaluation models have not conducted in-depth research on the evacuation potential of populations. Thus, limited guidance is available for relevant departments to formulate emergency plans to reduce the potential *LOL*. Therefore, a new comprehensive evaluation model was proposed in this study. According to the relevant references and disaster theory, the main influencing factors and the process through which the *LOL* is caused by dam breaches were determined. The specific occurrence process was divided into six stages: a dam breach causes flood, the flood puts the *PAR*, the *PAR* complete the preparation work, the *PAR* evacuate, the un-evacuated population shelter themselves inside buildings, and flood causes the death of the exposed population. To calculate the *LOL*, the parameters relevant at each stage were defined. Furthermore, the Hydrologic Engineering Center's River Analysis System, Geographic Information System, and related materials were used to simulate the flood routing and evacuation potential of the *PAR*, quantifying the parameters in the model. The model was applied to 14 towns in the downstream areas of the Luhun Reservoir in Henan Province, China, and its accuracy was verified by comparing the results obtained from the two existing models. In addition, the specific suggestions for reducing the potential *LOL* were proposed based on the results of the simulation.

1. Introduction

Dam service flood control, navigation, power generation, and irrigation have significant economic benefits (Latrubesse et al., 2017). However, once a dam breach occurs, it has disastrous consequences in downstream areas (Ge et al., 2020a; Pathak et al., 2020; Zeng et al., 2019). According to Li et al. (2019), China had an average of 57.9 dam breaches per year from 1954 to 2014. Although there has been significant improvement in the project quality and management level in recent years, dam breaches still occur from time to time owing to natural disasters, human factors, and strength loss caused by long-term disrepair. (Ge et al., 2020b; Thrysøe et al., 2021). In July 2018, at least 20 people were killed and more than 100 went missing owing to the flood caused by the collapse of a dam under construction, which was a part of the Xe-Pian Xe-Namnoy hydroelectric power project in southeast Laos (Kim and Lee, 2020). In August 2018, heavy rains caused the dam breach of the Sheyuegou Reservoir in Xinjiang, China, leading to 20 deaths and 8 missing (Beijing News, 2018). In May 2020, the Sardoba Reservoir in Sirdaryo Viloyati, Uzbekistan, broke because of a typhoon, and led to the evacuation of approximately 70,000 residents, 4 deaths, and 56 injuries (Xinhuanet, 2020). In May 2020, the Edenville Dam in the United States broke, due to its poor condition and heavy rainfall, causing more than 10,000 people forced to evacuate urgently. Consequently, the potential loss of life (*LOL*) caused by dam breaches has always attracted the attention of researchers. (Aboelata et al., 2003; Lumbroso et al., 2011, 2021; Johnstone and Garrett, 2014; Ge et al., 2017; Georges et al.,

* Corresponding author.
E-mail address: wumeimei@haut.edu.cn (M. Wu).

https://doi.org/10.1016/j.jhydrol.2022.128059
Received 7 November 2021; Received in revised form 24 May 2022; Accepted 9 June 2022
Available online 15 June 2022

2019).

Generally, empirical models, which established by regression analysis of historical dam breach events, were used to establish the functional relationship between the *LOL* and certain key parameters. Brown and Graham (1988) proposed a method for predicting the *LOL* based on the analysis of the population at risk (*PAR*) and the warning time (T_W). Considering the various levels of severity of dam breach flood, Dekay and McClelland (1993) proposed a formula for estimating the nonlinear relationship between the *LOL* and *PAR*. Graham (1999) added the degree of understanding of the dam breach to the influencing factors, and proposed the mortality of the *PAR*. Based on Graham (1999), Zhou et al. (2007) analyzed the data of eight dams in China, and established a corresponding assessment model of the *LOL* caused by dam breaches. The U.S. Department of the Interior, Bureau of Reclamation (2015), has proposed a new method to replace the Graham method to estimate the *LOL*. Despite their easy application, most empirical models often have limited use owing to the low availability of the historical dataset (Jonkman et al., 2008).

Recently, the physical models, which focus on the formation mechanism analysis of the *LOL*, have gradually become research hotspots. Assaf and Hartford (2002) developed a virtual reality approach (BC Hydro's Life Safety Model (LSM)) to deal with the problems of failure consequence analysis and emergency planning. Aboelata and Bowles (2008) established the LIFESim model to evaluate the *LOL* of Greater New Orleans. Lumbroso et al. (2011, 2021) applied the LSM model to Malapasset dam, Canvey Island and Brumadinho tailings dam, combined with Monte Carlo, accurately estimated the possible *LOL* and put forward effective emergency management measures. This kind of agent-based physical models can simulate countless possible scenarios that may be caused by flood, and make effective security decisions. However, this kind of models have high requirements for data and operation users.

Therefore, the comprehensive evaluation models have begun in prosperity. Jonkman et al. (2008) developed a new function related to mortality to estimate the *LOL* caused by flood disasters in low-lying areas. Ehsan (2009) developed an improved method for *LOL* estimation. In addition, he also discussed the definitions of two flood severity and proposed a new definition of flood severity by using the method of geometric aggregate (GA). Considering more factors affecting the *LOL* and the relationships among them, Peng and Zhang (2012) constructed the HURAM model based on the Bayes model. Based on data obtained from 14 dam failure cases in China, Huang et al. (2017) proposed a new method for estimating the *LOL* using a three-dimensional stratified sampling method. Li et al. (2018) analyzed the weights of the primary factors that affect the consequences of dam breaches, using set pair analysis and the variable fuzzy set theory. Considering the extensive changes and effects of the various factors, Ge et al. (2019, 2021) constructed a rapid evaluation model based on the catastrophe theory, and used the interval theory to effectively determine the possible upper and lower limits of *LOL* caused by dam breaches, rather than a certain value. These comprehensive evaluation models focus on the innovation and application of mathematical methods, improving the accuracy compared with the empirical models significantly. However, owing to the lack of in-depth analysis of the evacuation potential of the *PAR*, they are unable to quantify certain critical types of information as effectively as the physical models, such as the time required for evacuation, shortest roads that can be used for evacuation, and the effective evacuation positions, resulting in deficiencies in guiding the relevant departments to formulate emergency plans.

Therefore, in order to facilitate application and provide reference and basis for formulating emergency evacuation plan to reduce potential *LOL*, combined with flood routing simulation, a new comprehensive evaluation model was established to quantify evacuation potential, such as the time required for evacuation and the effective evacuation positions, while estimating *LOL* caused by a dam breach.

2. Materials and methods

2.1. Study areas

The Luhun Reservoir is located in Songxian County, Henan Province, China, on the upper reaches of the Yihe River, a tributary of the Yellow River. The Luhun Reservoir focuses on flood control, irrigation, power generation, water supply, and tourism. It has a capacity of 1.316 billion m^3, whose designed flood standard is a 1,000-year event, and the checking flood standard is a 10,000-year event. The primary dam is an earth-rock dam with a maximum height of 55 m, and the terrain from the dam site to Longmen Grottoes is primarily hilly and shallow, with open mountains on either side and flat terrain in the middle. Most residents live near rivers, and the others are sparsely distributed in mountainous areas far away from the rivers. Secondary and arterial roads constitute the main roads, whereas higher traffic capacity roads such as motorways, trunk roads, and primary roads are fewer. The downstream areas of Longmen Grottoes are the primary locations of schools, enterprises, and government agencies, with open terrain, dense population, and well-developed transportation, as shown in Fig. 1.

2.2. Analysis of LOL caused by dam breaches

Ehsan (2009) developed an improved method for *LOL* estimation, in which all main influencing factors were incorporated in a detailed manner for *LOL* estimation. Based on the Ehsan's model, an improved *LOL* evaluation model was proposed by using a different approach, which can not only accurately evaluate the *LOL*, but also put forward effective evacuation suggestions.

2.2.1. Analysis of influencing factors of LOL

The main factors were summarized from the papers of Ehsan et al. (2009, 2013, 2014), and then some factors were screened and replaced, according to our aim and actual situation. For example, when evacuating by walking, the F_{age} (age risk factor) and F_h (health risk factor) of the *PAR* affects the evacuation speed. However, due to the difficulty in quantifying the impact and the lack of detailed statistical data in the study area, the F_{age} and F_h were not taken into account in this study. Considering whether the factors are easy to quantify or not, the F_{ev} (ease of evacuation factor) was expressed by transportation modes (M_T) and transportation network (N_T), F_{mt} (material risk factor) and F_{st} (storey risk factor) were expressed by the vulnerability of buildings (V_B).

According to the disaster theory, the influencing factors were determined from three aspects, i.e., disaster-causing factors, disaster-affected bodies, and disaster-prone environments (Wu et al., 2021), ensuring that the selected influencing factors systematically and comprehensively reflect the *LOL*.

2.2.1.1. Disaster-causing factors. Disaster-causing factors refer to flood caused by dam breaches. The product of flood depth (D) and velocity (V) reflects flood severity (S_F) (Qi and Altinakar, 2012), and determines the mortality of the exposed population (POP_{exp}) to flood, which can be quantified by the mortality function (F_M) (Jonkman et al., 2008).

2.2.1.2. Disaster-affected bodies. Disaster-affected bodies refer to the *PAR*. Without the *PAR*, there would be no *LOL* regardless of the severity of the flood. In the case of flood, evacuation is the most effective choice for saving the population. According to Urbanik (2000), the *PAR* require a certain response time (T_R) to evacuate, which has a significant impact on the evacuation.

2.2.1.3. Disaster-prone environments. Disaster-prone environments refer to the environmental characteristic factors downstream, where the disaster-affected bodies are located. The warning time (T_W), transportation modes (M_T), and transportation network (N_T) are the key

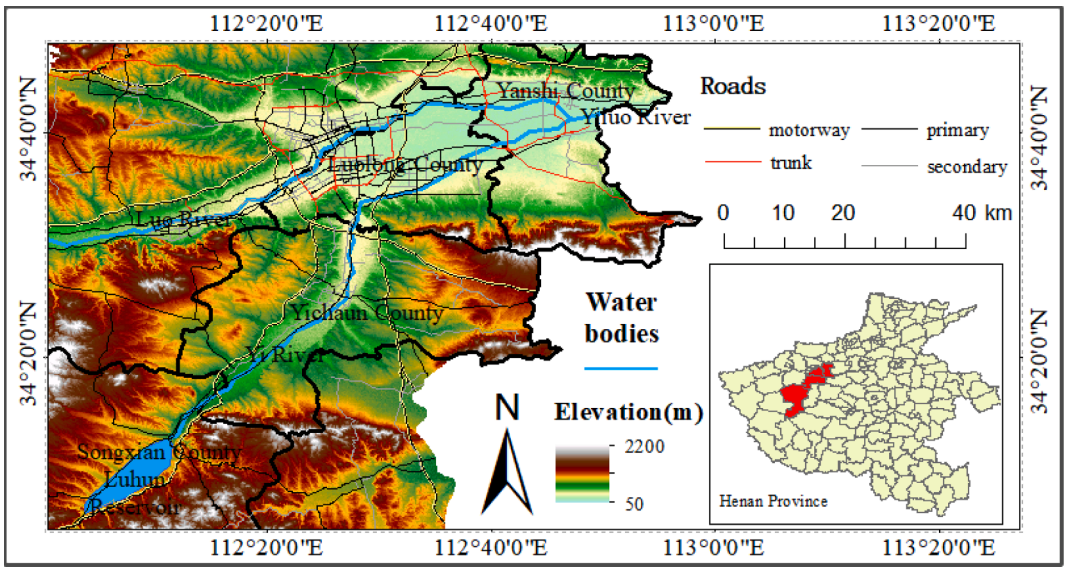

Fig. 1. General situation of study area.

factors that affect the evacuation of the *PAR* (Cheng et al., 2011). In addition, the downstream buildings provide the primary shelters for the *PAR*, thus, building vulnerability (V_B) is significant (Rescdam, 2000; Yang et al., 2021).

2.2.2. Analysis of the formation process of LOL

The process of *LOL* caused by a dam breach was determined based on the disaster-causing mechanism and the interrelationship among the influencing factors (Ge et al., 2021), as shown in Fig. 2.

Based on Fig. 2, the specific *LOL* process can be divided into six stages.

(1) A dam breach causes flood

Flood caused by damage to the dam body or auxiliary structures owing to overtopping, quality problems, improper management and so on pose significant threats to the safety of the downstream population.

(2) Flood puts *PAR*

The number of *PAR* is mainly related to the flood inundation areas and distribution state of the downstream population. According to Sun et al. (2014) and Penning-Rowsell et al. (2005), the residents located in the downstream potential submerged areas can be defined as the *PAR*.

(3) *PAR* complete the preparation work before evacuation

The preparation work of the *PAR* consists of two parts: receiving the warning and responding. The proportion of the population who have completed the preparation work to *PAR* can be defined as the preparedness rate (R_P). Therefore, the number of the population who have completed the preparation work (POP_{pre}) can be calculated by Eq. (1). The population who have not completed the preparation work becomes a part of the un-evacuated population ($POP_{un\text{-}eva}$).

$$POP_{pre} = PARR_P \tag{1}$$

(4) *PAR* evacuate from flood-affected areas

The proportion of the evacuated population (POP_{eva}) who have reached safe areas before the flood arrives to the POP_{pre} can be defined as the evacuation rate (R_E), as expressed in Eq. (2). Those who fail to evacuate to safe areas become another part of the $POP_{un\text{-}eva}$.

$$R_E = \frac{POPeva}{POPpre} \tag{2}$$

(5) $POP_{un\text{-}eva}$ shelter themselves inside buildings

The $POP_{un\text{-}eva}$ shelter themselves inside the surrounding buildings. Certain buildings resist the impact of flood successfully so that the people taking shelter can survive. The proportion of the population successfully sheltered (POP_{shel}) to $POP_{un\text{-}eva}$ can be defined as the shelter rate (R_S), which can be approximately expressed by the proportion of

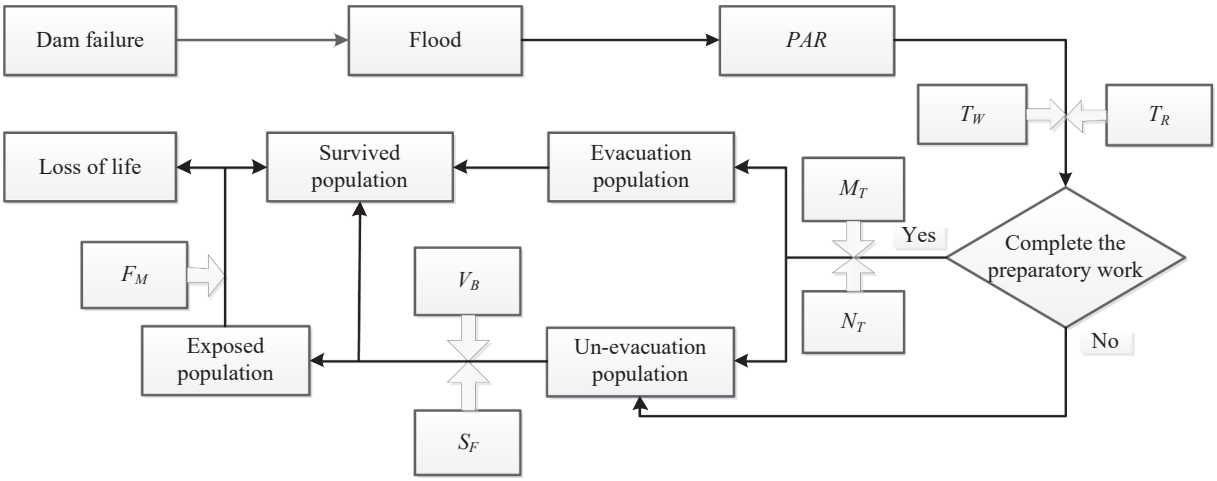

Fig. 2. Formation process of *LOL* caused by a dam breach.

damage to the buildings, as expressed in Eq. (3):

$$R_S = \frac{POP_{shel}}{POP_{un-eva}} = \frac{NUM_{un-dest}}{NUMtot} \tag{3}$$

where $NUM_{un\text{-}dest}$ is the number of buildings that successfully resist the impact of flood, and NUM_{tot} is the total number of buildings that face the flood, respectively.

(6) Flood causes the death of the POP_{exp}

The other buildings are destroyed, causing the population that has taken shelter in them to become the POP_{exp}. A portion of the POP_{exp} loses their lives owing to the flood. Setting F_M as the mortality of the POP_{exp}, the LOL can be calculated by Eq. (4):

$$LOL = POP_{\exp} F_M \tag{4}$$

According to Eq. (1) -Eq. (4), the LOL caused by a dam breach can be calculated by Eq. (5):

$$LOL = PAR(1 \ - -R_P R_E)(1 \ - -R_S)F_M \tag{5}$$

where PAR and F_M are determined by the flood caused by a dam breach, and R_P, R_E, R_S are used to describe the evacuation potential of the PAR under the threat of flood.

Therefore, an accurate simulation of the dam breach flood and the population evacuation potential are the foundation and key to estimating the LOL.

2.3. Simulation of Dam breach flood and their effects on LOL

2.3.1. Simulation of dam breach flood

The Hydrologic Engineering Center's River Analysis System (HEC-RAS) hydrodynamic model has been widely used because of its easy operation and complete function. It was developed by the Hydrologic Engineering Center of the US Army Corps of Engineers, and its primary functions include water surface line calculation of constant flow, unsteady flow simulation, sediment transport calculation of movable boundaries, and water quality analysis (United States Army Corps of Engineers, 2016). In this study, a two-dimensional model of unsteady flow was selected to simulate the dam breach flood.

The main dam of the Luhun Reservoir is an earth-rock dam. In general, three types of damage that lead to breaches in earth-rock dams are (Carrivick et al., 2011; Abdedou, et al., 2020): (a) overtopping caused by excessive flood during the monsoons; (b) seepage, piping, and other factors under regular water level conditions during the non-flood season; and (c) certain other factors, for example, earthquakes and wars. Relevant statistics indicate that overtopping is the primary cause for the breach of an earth-rock dam (Zhao et al., 2020). Furthermore, as these dams are broken gradually, most breaches are transverse partial ones (Peter et al., 2018; Walder et al., 2015; Lee, 2019). Currently, there is no authoritative estimation method for the vertical breach height (Wang et al., 2018). For safety, the worst situation of breaching at the bottom of the dam was considered. Therefore, the simulation condition of the Luhun Reservoir dam breach was set as follows: overtopping caused a dam breach with horizontal local and vertical dam breaks to the bottom. While simulating the flood caused by a dam breach, the effects of various types of land on flood routing were also considered. The downstream terrain was divided into 50 m × 50 m computational grids and the Manning coefficient (n) was assigned (Dazzi et al., 2019; Chen et al., 2020).

2.3.2. Determination of the Number of the PAR

The number of PAR primarily depends on the area submerged by the dam breach flood and the distribution of the population in the submerged areas. Where the reservoir capacity is small or the population density is low, the PAR in the downstream inundation area is relatively small. Hence, in many countries or regions, the PAR distribution at various times and seasons can be obtained through typical surveys and census data. However, for the Luhun Reservoir with a capacity of 1.316 billion m^3, it is difficult to analyze the population distribution of each place in detail because of the large potential submerged areas. Therefore, the PAR in a certain area can be regarded as a point, and the total PAR can be obtained by determining the population at each point (Zhou et al., 2007), as expressed in Eq. (6).

$$PAR = \sum_{i=1}^{n} PARi \tag{6}$$

where n is the number of submerged settlements, and PAR_i is the size of the population in the ith settlement.

2.3.3. Determination of the Mortality of the POP_{exp}

The mortality of POP_{exp} approximately follows a normal distribution. Based on the characteristics of the flood, the inundated areas were divided into the breach zone (zone I), zone with rapidly rising water (zone II), and remaining zone (zone III). Each zone had a corresponding mortality function, F_M (Jonkman et al., 2008).

(a) Breach zone.

Owing to the high flow velocities and forces, the flood in such areas is extremely destructive. When $S_F \geq 7\ m^2/s$ and $V \geq 2$ m/s, the buildings will collapse and people will lose their stability simultaneously. F_M can be considered a constant value, as expressed shown in Eq. (7):

$$F_M = 1 \tag{7}$$

(b) Zone with rapidly rising water.

The flood intensity in such areas is lower than that in zone I. The POP_{exp} has the potential to survive, but it is significantly affected by the flood rising speed (S_R). When $S_R > 0.5$ m/h, people have little time to escape because the rapid increase in the level of water is particularly hazardous. According to Peng et al. (2012), $D \geqq 2.1$ m and $S_R > 0.5$ m/h are the lower limits of zone II, and the corresponding F_M can be calculated by Eq. (8):

$$FM = \Phi N\left(\frac{\ln D - 1.46}{0.28}\right) \tag{8}$$

where ΦN is the cumulative normal distribution function.

(c) Remaining zone.

In such areas, the flood intensity is significantly weakened and the probability of people's survival is likely to be higher. The corresponding F_M can be calculated by Eq. (9):

$$FM = \Phi N\left(\frac{\ln D - 7.6}{2.75}\right) \tag{9}$$

where ΦN is the cumulative normal distribution function.

2.4. Simulation of evacuation potential of PAR

2.4.1. Determination of the R_P

People receive warning messages from various channels, such as the government, relatives and friends, electronic media, radio, and social software. Therefore, a certain warning time (T_W) is required. In addition, after receiving the warning, a certain response time (T_R) is also required for people to notify their relatives and friends, return home from work, wait for the family members, and pack luggage (Kuller et al., 2021). It was assumed that the probability distributions of these two events were mutually independent, and the probability of each successive event relied on the probability distribution of the activities that preceded it. Thus, the probability of completing the two events is equal to the product of the probabilities of completing each event, as shown in Table 1 (Urbanik, 2000; Xue et al., 2019).

Based on Table 1, $t = 15$ min may be composed of 5 min of receiving warning time and 10 min of response time, or 10 min of receiving warning time and 5 min of response time. Therefore, the probability of t

Table 1
Probability product distributions of warning time T_W and response time T_R.

			T_R distribution					
			$t = 5$ $P(t) = 0.15$	$t = 10$ $P(t) = 0.15$	$t = 15$ $P(t) = 0.30$	$t = 20$ $P(t) = 0.15$	$t = 25$ $P(t) = 0.15$	$t = 30$ $P(t) = 0.10$
T_W distribution	$t = 5$	$P(t) = 0.2$	0.03	0.03	0.06	0.03	0.03	0.02
	$t = 10$	$P(t) = 0.4$	0.06	0.06	0.12	0.06	0.06	0.04
	$t = 15$	$P(t) = 0.4$	0.06	0.06	0.12	0.06	0.06	0.04

= 15 min is the sum of these two possibilities. The probability of other values of t can be determined similarly, and the probability distribution of R_P can be obtained by accumulation, as shown in Table 2.

2.4.2. Determination of the R_E of PAR

Evacuation is a complicated process that is impacted by various factors such as traffic conditions, evacuation methods, and evacuation routes (Cheng et al., 2011). The population distribution and shelter location in residential areas were simplified as points, and the local roads were simplified as lines. Considering the submerged residential areas as the starting points and the evacuation positions that are not submerged as the end points, an OD (Origin- Destination) matrix was established in the GIS. Time is the primary consideration in the process of emergency evacuation. Thus, the matrix was solved at the cost of time.

In developed countries, most residents are evacuated by their own private cars (Fm et al., 2018). However, in China, owing to low private car ownership, a large number of residents have to choose other means of evacuation. In addition, dam failure usually occurs suddenly. In extreme circumstances, the government may not have enough time to organize an evacuation. Therefore, it was assumed that the *PAR* can evacuate by cars, motorcycles, and bicycles as well as by walking.

The evacuation time is related to the road capacity and traffic conditions. Based on an investigation on a large number of road sections, The Bureau of Public Roads (2009) of the United States of America obtained the functional relationship between driving time and the traffic load, i.e., the *BPR* function, as expressed in Eq. (10):

$$t = t0\left[1 + \alpha\left(\frac{Q}{C}\right)^{\beta}\right] \tag{10}$$

where t is the driving time of the vehicle on the road section, t_0 is the driving time of the free flow of the road section, Q is the traffic flow of the road section, C is the design capacity of the road section, $\alpha = 0.15$, and $\beta = 4.0$.

During the process of evacuation, the traffic lights at the intersections are mainly controlled by the government, which can be ignored. However, pedestrians crossing the road may cause a greater disturbance to the traffic. Therefore, the coefficient μ was used to correct v_0, as expressed in Eq. (11) and Eq. (12).

$$t_0 = \frac{l}{v} \tag{11}$$

Table 2
Distribution of R_P.

t/min	Probability of each time period/%	R_P/%
5	0	0
10	3	3
15	9	12
20	18	30
25	21	51
30	19	72
35	14	86
40	10	96
45	4	100

$$v = \mu \cdot v_0 \tag{12}$$

where l is the length of the road section, v is the driving speed on the road section l, μ is the pedestrian interference coefficient, and v_0 is the design speed of the road section. The value standard of μ is shown in Table 3 (Cheng et al., 2011).

Without any interference, the average speeds of walking, cycling, and motorcycle evacuation are 6, 16, and 50 km/h, respectively (Wang and Song, 2014). However, owing to the poor traffic capacity of certain roads, it is often difficult to reach the ideal speed. Therefore, the road speed limit, which has a significant relationship with the traffic capacity, was set as the upper limit of the evacuation speed. For example, when driving on a road with a speed limit of 20 km/h, evacuees can reach the ideal average speed of walking or cycling, whereas while riding a motorcycle, they can only reach a maximum speed of 20 km/h. The evacuation time required on each road can be determined by dividing the length of the road by the average driving speed on it.

If the available time is longer than the required time, that is, the flood arrival time – (warning time + response time) > time required for evacuation, the population can be considered to evacuate successfully. Hence, R_E can be calculated by Eq. (2).

2.4.3. Determination of the R_S of $POP_{un\text{-}eva}$

In areas where buildings collapse or safe shelters cannot be provided, significant *LOL* may occur. The *PAR* require a short time to shelter themselves inside their own or nearby buildings. Therefore, it can be assumed that they have been evenly distributed among the buildings before the flood arrives. Whether a building is damaged or not is mainly determined by flood intensity and building vulnerability. The RESCDAM project (2000) tested the damage caused to buildings in flood and proposed standards accordingly. Wang and Song (2014) established China's building damage standard based on the relevant results, as shown in Table 4.

According to Table 4, the vulnerability of buildings is mainly related to their constituent materials and floors. Material information can be obtained through satellites, remote sensing data, or surveys in the study area. The floor information can be converted from the building vector data. The building vector data include the underside contour and height spatial distribution information, which can be converted into floor information based on the corresponding criteria (Yu and Wen, 2016), as shown in Table 5.

Whether the buildings were damaged or not can be determined based on the superimposition of the building vector data, which have been converted into layers, with the flood division based on the building damage criteria specified in the GIS. It is worth noting that one building may be in multiple damaged areas simultaneously, and it should be judged based on the most unfavorable situation. For example, in three-story building destruction areas, buildings with three floors or less will be destroyed, and buildings with more than three floors will not be

Table 3
Correction coefficient value of pedestrian interference.

Degree of interference	Extremely serious	Serious	Moderate	General	Slight	None
μ	0.5	0.6	0.7	0.8	0.9	1.0

Table 4
Reference standards for buildings damage in China.

Building type	Damage standards for buildings	
Mud bungalows		$D \geq 0.9$ m and $S_F \geq 2$ m^2/s
Brick and concrete	Bungalows	$V \geq 2$ m/s and $S_F \geq 7$ m^2/s
	Two-story buildings	$V \geq 2.4$ m/s and $S_F \geq 15$ m^2/s
	Three-story buildings	$V \geq 2.4$ m/s and $S_F \geq 22$ m^2/s
	Four-story buildings	$V \geq 2.54$ m/s and $S_F \geq 29$ m^2/s

Note: For the buildings higher than four stories, their ability to resist flood is very strong, which can be considered that not to be damaged.

Table 5
Transformation rule of buildings' heights to floors in the study area.

Height (m)	≤4	5–7	8–10	11–13
Floors	1	2	3	4

destroyed. A two-story building is considered to be damaged if it is in the damaged area of both two-story and three-story buildings.

The number of buildings destroyed in each residential area can be counted using the frequency statistics function of the GIS. Therefore, the R_S of the $POP_{un\text{-}eva}$ can be calculated by Eq. (3).

3. Results

3.1. Simulation results of dam breach flood

Based on the simulation results of dam breach flood, the maximum width of the breach is reached after 1.35 h, final bottom width is 165 m, and maximum flow of the breach is 57,769 m^3/s. The flood reached Yichuan County after 0.8 h and Longmen Grottoes in Luolong County after 3.6 h. In the Longmen Grottoes region, affected by its narrow valley and low-lying terrain, the water depth reached a maximum of approximately 29 m, and the flow velocity in the center of the river increased sharply to approximately 23 m/s. Beyond Longmen Grottoes, owing to the flat and open terrain downstream, the flood begins to spread and the flow velocity gradually slows down, and it reaches Yanshi County after 8.7 h. The total submerged area in Luoyang is approximately 291 km^2, primarily involving 14 residential areas in Songxian County, Yichuan County, Luolong County, and Yanshi County. The locations listed in the order of their distances from the dam site from near to far are as follows: Minggao Town (A), Baiyuan Town (B), Chengguan Town (C), Pengpo Town (D), Longmen Grottoes left bank (E), Longmen Grottoes right bank (F), Longmen Town (G), Zhuge Town (H), Taikang east road (I), Lilou Town (J), Dianzhuang Town (K), Pangcun Town (L), Zhai Town (M), and Yuetan Town (N). The inundation situation is shown in Fig. 3.

3.2. Simulation results of PAR evacuation potential

The ownership rate of private cars in Luoyang City, where the Luhun Reservoir is located, is 19.6%. According to Cova and Johnson (2015), each car can take two to three people (2.5 is selected). Owing to the lack of detailed statistics, it was assumed that the residents give priority to cars, whereas the remaining people were evacuated on average using motorcycles and bicycles and by walking. Thus, the proportion of residents evacuated using cars was 49%, and that for the other three methods was 17%. The time required for evacuation of the *PAR* in each town was calculated by the OD matrix, as shown in Fig. 4.

Three conditions were assumed: each town issued a warning message 0, 0.5, and 1 h before the flood arrived. By combining the time required for evacuation, the maximum time allowed for the population to complete the preparation work can be calculated. At this time, the corresponding preparation rate R_P is the proportion of the *PAR* that can be successfully evacuated, that is the R_E.

Through information from the building vector data converted into

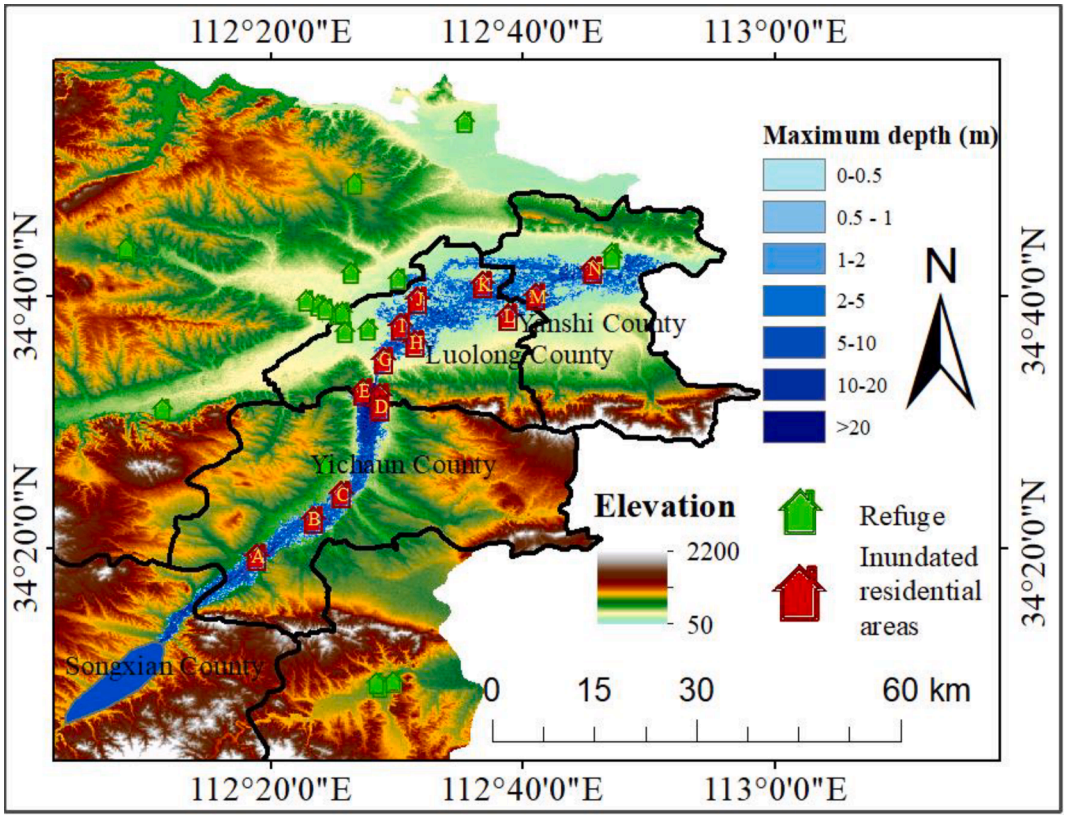

Fig. 3. Inundation of the reservoir downstream.

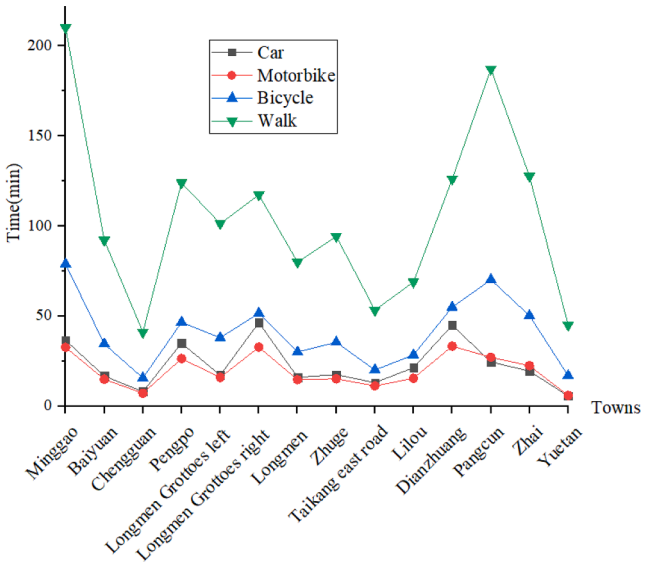

Fig. 4. Required time for towns to evacuation.

floors, it was found that there were almost no bungalows in the submerged area. Nowadays, buildings in the downstream area are all constructed from either bricks or concrete. Taking Chengguan Town of Yichuan County as an example, the damage to the buildings in this area is shown in Fig. 5, and the R_S can be calculated by Eq. (3).

3.3. Results of estimation of LOL

Based on the results of simulation of flood routing and population evacuation potential, the results of estimation of the *LOL* in each town are shown in Table 6.

4. Discussion

4.1. Comparison with Ehsan's model

Ehsan (2009) proposed a method for calculation *LOL*, as expressed in Eq. (13).

$$LOL_i = PAR_i \times FAT_{BASE} \times F_{sv} \times F_{age} \times F_{mt} \times F_{st} \times F_h \times F_{war} \times F_{ev} \quad (13)$$

where LOL_i = loss of life at a particular location " i" downstream of the dam, PAR_i = population at risk at a particular location " i" downstream of the dam, FAT_{BASE} = Base fatality rate of 0.15, F_{sv} = Flood severity factor, F_{age} = Age risk factor, F_{mt} = Material risk factor, F_{st} = Storey risk factor, F_h = Health risk factor, F_{war} = Warning factor, F_{ev} = Ease of evacuation factor.

Ehsan's model was applied to the case of this study to calculate the *LOL* under different warning time. The value of the coefficients and the results of *LOL* are shown in Table 7.

Comparison between the estimation results of Ehsan's model and the proposed model was made, as shown in Table 8.

According to Table 8, the mortality of the proposed model is larger than the Ehsan's model, which is caused by the following reasons:

(a) Due to the different national conditions, the models of other countries are not necessarily suitable for direct application to China. For example, in the Ehsan's method, the value of F_{ST} is:

$$Fst = 1 (for\ high\ severity\ and\ all\ types\ of\ houses) \quad (14)$$

$$Fst = 1 - -S\%\ (for\ medium\ and\ low\ severity) \quad (15)$$

where S = % of more story houses.

However, there may be great differences in the standards of the

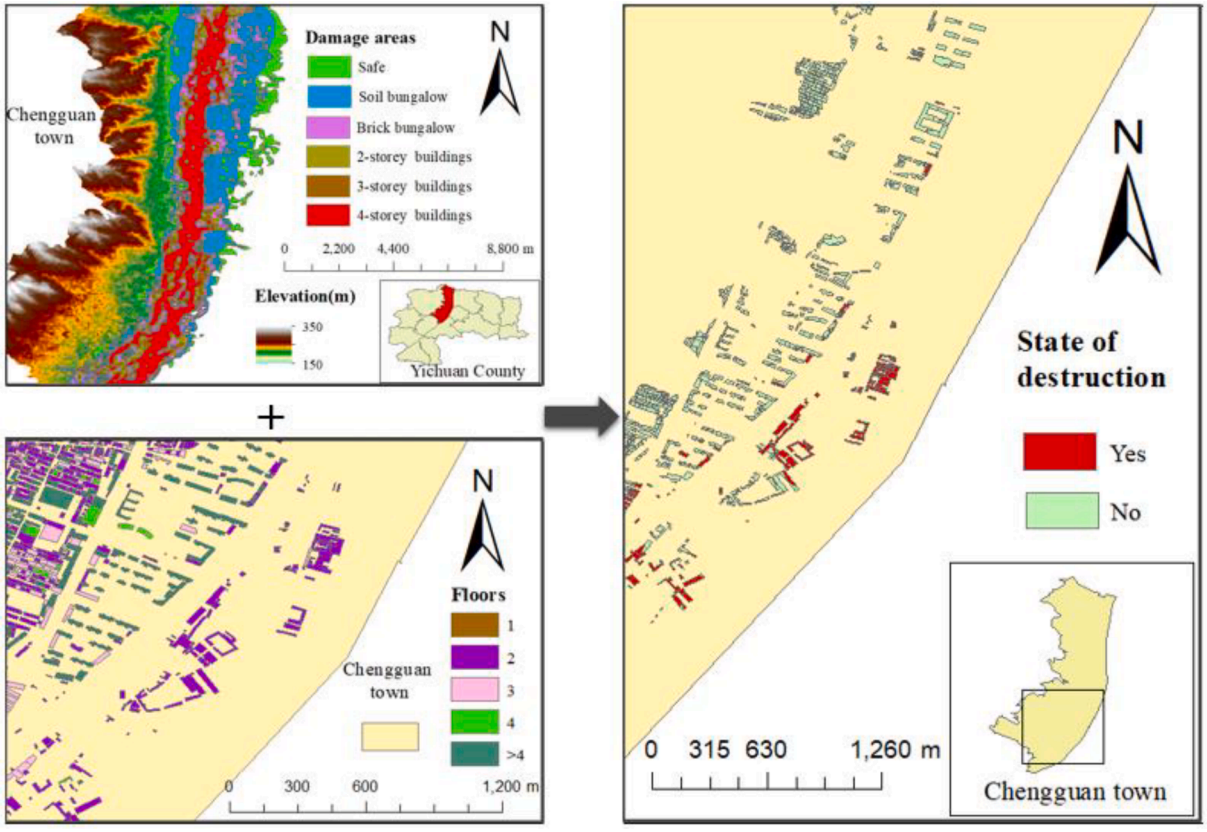

Fig. 5. Damage of buildings in Chengguan Town.

Table 6
Results of estimation of *LOL* in 14 downstream towns.

Towns		*PAR*	R_E T_W/hour			R_S/%	Mortality zone	F_M	*LOL* T_W/hour		
			0	0.5	1				0	0.5	1
A	Minggao	8614	0	0	31.518	61.670	I	1.000	3302	3302	2261
B	Baiyuan	12,527	0	6.588	74.104	55.001	I	1.000	5637	5370	1460
C	Chengguan	21,982	0	27.472	87.390	72.730	I	1.000	5994	4809	756
D	Pengpo	10,569	0	0	40.108	67.331	II	0.781	2697	2697	1615
E	Longmen Grottoes left bank	6360	0	5.519	71.415	68.319	iii	0.033	66	64	19
F	Longmen Grottoes right bank	3465	0	0	15.094	69.301	iii	0.028	30	30	25
G	Longmen	4032	0	7.564	73.140	63.674	I	1.000	1465	1385	393
H	Zhuge	10,302	0	5.552	73.287	81.853	II	0.113	141	136	38
I	Taikang east road	7426	0	12.295	82.454	77.309	II	0.127	10	9	2
J	Lilou	29,551	0	3.110	75.181	64.909	iii	0.032	332	324	80
K	Dianzhuang	20,528	0	0	16.334	73.208	II	0.837	4603	4603	3851
L	Pangcun	8405	0	0.100	56.181	91.422	iii	0.007	5	5	2
M	Zhai	31,043	0	1.820	63.357	71.063	iii	0.005	45	44	16
N	Yutan	20,215	0	17.042	85.471	69.660	iii	0.021	129	113	19

Table 7
Estimation results of Ehsan's model.

Towns	*PAR*	F_{sv}	F_{st}	F_{war}(min)			F_{ev}(min)			*LOL*		
				0	30	60	0	30	60	0	30	60
A	8614	1	1	1	0.7	0.3	1	0.7	0.3	1034	507	93
B	12,527	1	1	1	0.7	0.3	1	0.7	0.3	1503	737	135
C	21,982	1	1	1	0.7	0.3	1	0.7	0.3	2638	1293	e
D	10,569	0.3	0.01	1	0.7	0.3	1	0.7	0.3	4	2	0
E	6360	0.3	0.01	1	0.7	0.3	1	0.7	0.3	2	1	0
F	3465	0.3	0.01	1	0.7	0.3	1	0.7	0.3	1	1	0
G	4032	1	1	1	0.7	0.3	1	0.7	0.3	484	237	44
H	10,302	0.3	0.01	1	0.7	0.3	1	0.7	0.3	4	2	0
I	7426	0.3	0.01	1	0.7	0.3	1	0.7	0.3	3	1	0
J	29,551	0.3	0.01	1	0.7	0.3	1	0.7	0.3	11	5	1
K	20,528	0.3	0.01	1	0.7	0.3	1	0.7	0.3	7	4	1
L	8405	0.3	0.01	1	0.7	0.3	1	0.7	0.3	3	1	0
M	31,043	0.3	0.01	1	0.7	0.3	1	0.7	0.3	11	15	1
N	20,215	0.3	0.01	1	0.7	0.3	1	0.7	0.3	7	4	1

Table 8
Comparison between the estimation results of Ehsan's model and the proposed model.

Towns	Mortality of Ehsan's model			Mortality of the proposed model		
	0 min	30 min	60 min	0 min	30 min	60 min
A	12.00	5.88	1.08	38.33	38.33	26.25
B	12.00	5.88	1.08	45.00	42.87	11.65
C	12.00	5.88	1.08	27.27	21.88	3.44
D	0.04	0.02	0.00	25.52	25.52	15.28
E	0.04	0.02	0.00	1.04	1.01	0.30
F	0.04	0.02	0.00	0.87	0.87	0.72
G	12.00	5.88	1.08	36.33	34.35	9.75
H	0.04	0.02	0.00	1.37	1.32	0.37
I	0.04	0.02	0.00	0.13	0.12	0.03
J	0.04	0.02	0.00	1.12	1.10	0.27
K	0.04	0.02	0.00	22.42	22.42	18.76
L	0.04	0.02	0.00	0.06	0.06	0.02
M	0.04	0.02	0.00	0.14	0.14	0.05
N	0.04	0.02	0.00	0.64	0.56	0.09

construction industry, the structure and materials of houses in different countries. Therefore, when judging the damage of houses in the flood, the standards for houses damage in China (as shown in Table 4) were used in the proposed model, which led to the difference in the evaluation results between the proposed model and Ehsan's model.

(b) When Ehsan's model was used to calculate the *LOL* in study case, $F_{sv} = 0.3$ was taken in all medium flood severity areas. However, the special topography of Luhun reservoir leads to more serious flood. The flood severity in many areas is of medium severity, but very close to high severity. At this time, $Fsv = 0.8$ or 0.9 is more suitable. The proposed model took this situation into account in more detail, so the results are larger than Ehsan's model. Furthermore, the proposed model is more sensitive to water depth (D). In the same flood severity areas, the value of FAT_{BASE} in Ehsan's model is the constant, but the value of F_M in the proposed model increases with the increasement of D. Therefore, based on the proposed method, the calculation results of Luhun Reservoir with deep flood in the downstream are larger.

(c) Ehsan's model lays the foundation for the accurate assessment of *LOL*. Combined with the above comparison, it is suggested that when using the Ehsan's model, the selection of parameters can be analyzed more carefully, so as to further improve the accuracy of the results.

4.2. Comparison with Li-Zhou model

Based on the actual situation prevailing in China, considering the Graham method and certain other influencing factors, Zhou et al. (2007) presented the mortality table of the *PAR* for estimating the *LOL* caused by dam breaches in China. The results of estimation obtained from the model proposed in this study were compared with those of Li-Zhou model, as shown in Table9.

According to Table 9, when the warning time for Town B is 0.5 h and those of Towns J and N are 0 h, the estimation results are not within the scope of the Li-Zhou model. However, this situation can be attributed to specific reasons. Town B (Baiyuan Town) is a rural area, where the proportion of houses with more floors is much lower than that in urban areas. Only approximately 55% of the houses could effectively resist flood in the area. Hence, most of the $POP_{un\text{-}eva}$ are exposed to the flood,

Table 9
Comparison between the results of the proposed model and Li-Zhou model.

Severity of flood	Towns	T_W/ h	Mortality /%	
			The proposed model	Li-Zhou model
High ($S_F > 12$ m^2/s)	ABCG	0	38.3345.0027.2736.33	(10100)
		0.5	38.3342.8621.8834.35	(040)
		1	26.2511.653.449.76	(040)
Medium ($S_F >$ 4.6 m^2/s)	DHIJKN	0	25.512.052.881.1222.420.64	(280)
		0.5	25.511.972.631.1022.420.56	(0.0527)
		1	15.280.550.510.2718.760.09	(0.0527)
Low ($S_F \leq 4.6$ m^2/s)	EFLM	0	1.050.860.060.14	(05)
		0.5	1.000.860.060.14	(01.5)
		1	0.300.730.030.05	(01.5)

leading to a significant *LOL*. The values of S_F for Towns J (Lilou Town) and N (Yuetan Town) are medium, primarily because of its large water depth. However, the flow velocity is small, and the impact of the flood on the houses and the POP_{exp} is limited. Thus, it will not cause serious casualties. The results of the estimation for other towns under various warning times are all within the scope of the Li-Zhou model, which verifies the accuracy of the proposed model.

4.3. Analysis of the simulation results

(a) According to Fig. 4, Town A (Minggao Town) and Town L (Pangcun Town) require the maximum amount of time for complete evacuation, at 210 and 187 min, respectively. Town A is closest to the dam site among the 14 residential towns. The dam breach flood arrives within 50 min, which is far less than the time required for evacuation. Therefore, the relevant departments should prioritize the evacuation. Town L is far from the dam site, and the flood arrives late. If the early warning is timely, the population will have sufficient time to evacuate. The time required for complete evacuation of other towns is within 130 min, and the longest is 128 min. Among these, the towns with longer evacuation times are Town D (Pengpo Town), Town F (Longmen Grottoes right bank), Town K (Dianzhuang Town), and Town M (Zhai Town), which take 124, 117, 126, and 128 min, respectively. To reduce the potential *LOL* as much as possible, the relevant departments should issue early warnings and properly arrange the evacuation sequence for residents based on the flood arrival time and the amount of time required for evacuation.

(b) It is worth noting that if a flood disaster occurs, most residents in Luolong County will be evacuated to Hetaoyuan Park, Luopu Park, Luolong, and Luoyang Sports Center (the red positions displayed in Fig. 6), which may cause overcrowding. It is recommended that after properly attending to the injured, some people should be transferred to nearby locations, such as Mangshan Sports Park, Peony Park, Xiyuan Park, Peony Square, and the Shangyang Branch of Wangcheng Primary School (the blue positions displayed in Fig. 6). In addition, Fig. 3 indicates that Yichuan County has less capacity for receiving evacuees than Luolong County, which makes it inconvenient for the evacuation. Therefore, the relevant departments should set up temporary camps in the surrounding unsubmerged highlands to provide living supplies and medical assistance to asylum seekers.

(c) As compared with the existing methods, this model can not only estimate the *LOL* caused by dam breaches but also quantify significant information, such as evacuation time and effective shelter location, to facilitate the relevant departments in formulating effective evacuation strategies. In addition, unexpected situations may occur in the actual evacuation process, such as road obstruction or impassability owing to traffic accidents, broken trees and falling stones, and prohibited areas owing to the location of chemical enterprises, prisons, or military bases. To handle the impact of these emergencies, measures such as road blocking or traffic bans can be set up at the corresponding positions of the vector data in the GIS.

(d) The results of the estimation obtained from the proposed model are significantly affected by the accuracy of the flood characteristics. Because of the significant effects of the breach parameters and downstream roughness on the accuracy of the flood simulation, parameter

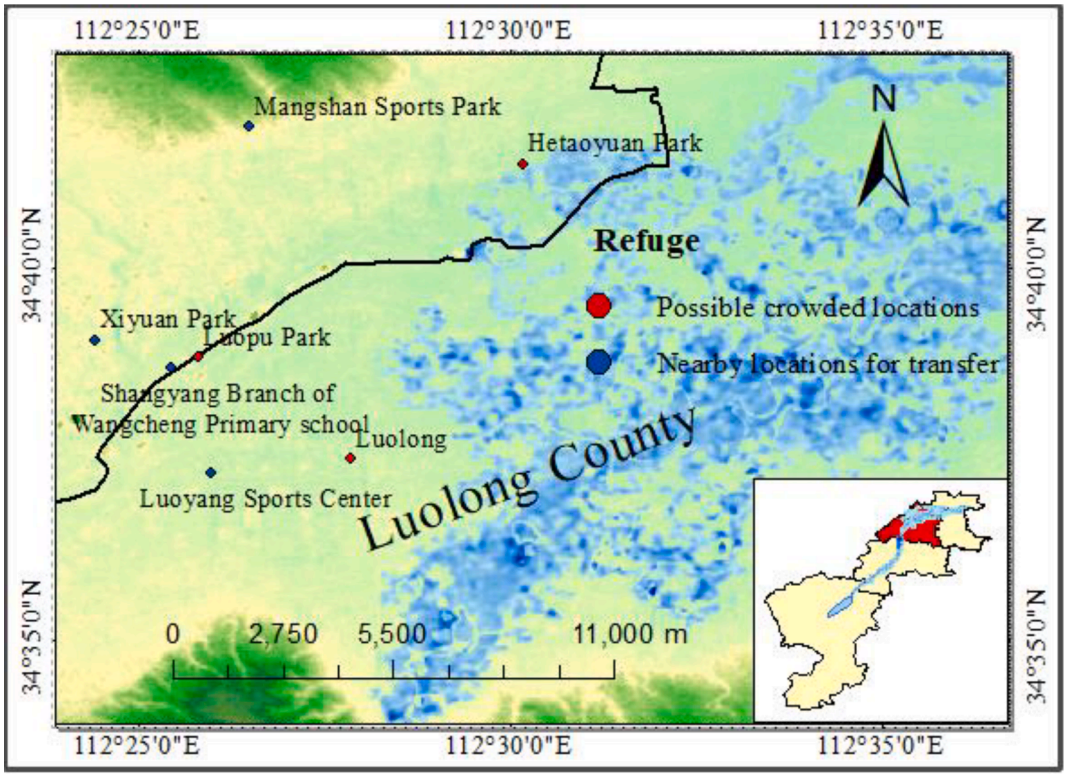

Fig. 6. Possible crowded locations and nearby locations for transfer.

selection and processing should be adjusted based on the specific conditions. Further, extreme weather, such as rainstorms, fog, and hail, has an adverse impact on the evacuation of the *PAR*, and the model can be further refined in combination with other relevant studies.

5. Conclusion

According to the analysis of influencing factors and formation process of *LOL*, a new comprehensive evaluation model was proposed, in which the parameters were quantified based on flood routing and population evacuation potential simulation. The HEC-RAS was used to simulate the flood caused by dam breaches and determine the number of *PAR* and the mortality of the POP_{exp}. The GIS and related vector data were used to simulate the evacuation potential of *PAR*, in which the R_P, R_E and R_S were quantified. Taking 14 towns downstream of the Luhun Reservoir in Luoyang, China, as an example, the estimation results of the proposed model were compared with those obtained from the two existing methods, indicating that the proposed model can effectively determine the potential *LOL* caused by dam breaches in China, which provides a reference for the relevant departments to formulate emergency plans.

CRediT authorship contribution statement

Wei Ge: Conceptualization, Formal analysis, Writing – review & editing. **Yutie Jiao:** Conceptualization, Formal analysis, Writing – original draft. **Meimei Wu:** Conceptualization, Methodology, Validation, Formal analysis, Writing – original draft. **Zongkun Li:** Methodology, Investigation, Funding acquisition. **Te Wang:** Methodology, Writing – review & editing. **Wei Li:** Validation, Supervision. **Yadong Zhang:** Validation. **Weixing Gao:** Investigation, Funding acquisition. **Pieter van Gelder:** Supervision.

Declaration of Competing Interest

The authors declare that they have no known competing financial interests or personal relationships that could have appeared to influence the work reported in this paper.

Acknowledgements

This research was supported by the National Natural Science-Foundation of China (Grant No. 52079127, 52179144, U2040224, 51679222, 51709239), the Fund of National Dam Safety Research Center (Grant No. CX2021B01), Program for Science & Technology Innovation Talents in Universities of Henan Province (HASTIT) (Grant No. 22HASTIT011), the Young Talent Support Project of Henan Province (Grant No. 2021HYTP024), and the Programs for Science and Technology Development of Henan Educational Committee (Grant No. 202102310394).

References

Aboelata, M., Bowles, D.S., Mcclelland, D.M., 2003. GIS model for estimating dam failure life loss. Risk. Anal. https://ascelibrary.org/doi/abs/10.1061/40694(2003)11.

Assaf, H., Hartford, D.N.D., 2002. A virtual reality approach to public protection and emergency preparedness planning in dam safety analysis. In Proceedings of the Canadian Dam Association Conference, Victoria, BC, Canada, 6–10 October.

Aboelata, H., Bowles, D.S, 2008. LIFESim: A tool for estimating and reducing life-loss resulting from dam and levee failures. In proceedings of the Association of State Dam Safety Officials (Dam Safety 2008), association of State Dam Safety Officials, Indian Wells, CA, America, 7–11 September.

Abdedou, A., Soulamani, A., Tchamen, G.W., 2020. Uncertainty propagation of dam break flow using the stochastic non-intrusive B-splines Bézier elements-based method. J. Hydrol. 590, 125342 https://doi.org/10.1016/j.jhydrol.2020.125342.

Beijing News, 2018. Flood caused by torrential rain in Hami, Xinjiang: 20 people were killed due to partial dam failure of the reservoir. http://news.sina.com.cn/c/2018-08-04/doc-ihhehtqh7551081.shtml.

Brown, C.A., Graham, W.J., 1988. Assessing the threat to life from dam failure. Water Resour. Bull. 24 (6), 1303–1309. https://doi.org/10.1111/j.1752-1688.1988.tb03051.x.

Bureau of Public Roads, 2009. Traffic assignment manual. US Department of Commerce. Urban Planning Divisions, Washington.

Cheng, C., Qian, X., Zhang, Y., Wang, Q., Sheng, J., 2011. Estimation of the evacuation clearance time based on dam-break simulation of the Huaxi dam in Southwestern China. Nat. Hazards. 57 (2), 227–243. https://doi.org/10.1007/s11069-010-9608-4.

Carrivick, J.L., Jones, R., Keevil, G., 2011. Experimental insights on geomorphological processes within dam break outburst floods. J. Hydrol. 408 (1–2), 153–163. https://doi.org/10.1016/j.jhydrol.2011.07.037.

Chen, C., Zhang, L., Xiao, T., He, J., 2020. Barrier lake bursting and flood routing in the Yarlung Tsangpo Grand Canyon in October 2018. J. Hydrol. 583, 124603 https://doi.org/10.1016/j.jhydrol.2020.124603.

Cova, T.J., Johnson, J.P., 2015. A network flow model for lane-based evacuation routing. Transp. Res. Part A 37 (7), 579–604. https://doi.org/10.1016/S0965-8564(03)00007-7.

DeKay, M.L., McClelland, G.H., 1993. Predicting LOL in cases of dam failure and flash flood. Risk Anal. 13 (2), 193–205. https://doi.org/10.1016/0167-6687(93)90920-K.

Dazzi, S., Vacondio, R., Mignosa, P., 2019. Integration of a levee breach erosion model in a GPU-accelerated 2D shallow water equations code. Water Resour. Res. 55 (1), 682–702. https://doi.org/10.1029/2018WR023826.

Ehsan, S., 2009. Evaluation of life safety risks related to severe flooding. Book (International edition), Institute of Hydraulic Engineering, Universität Stuttgart, Germany. Vol. 180.

Ehsan, S., Marx, W., Wieprecht, S., 2013. Estimation of flood warning times for flood safety management downstream of dams. J. River Eng. 1 (2).

Ehsan, S., Marx, W., 2014. Assessment of the possible extent of loss of life (LOL) downstream of large dams due to dam failure flooding. J. River Eng. 2 (5).

Ge, W., Sun, H., Zhang, H., Li, Z., Guo, X., Wang, X., Qin, Y., Gao, W., Van Gelder, P., 2020a. Economic risk criteria for dams considering the relative level of economy and industrial economic contribution. Sci. Total Environ. 725, 138–139. https://doi.org/10.1016/j.scitotenv.2020.138139.

Ge, W., Qin, Y., Li, Z., Zhang, H., Gao, W., Guo, X., Song, Z., Li, W., van Gelder, P., 2020b. An innovative methodology for establishing societal life risk criteria for dams: a case study to reservoir dam failure events in China. Int. J. Disast. Risk Re. 49, 101663.

Ge, W., Li, Z., Liang, R., Li, W., Cai, Y., 2017. Methodology for establishing risk criteria for dams in developing countries, case study of China. Water Resour. Manag. 31 (13), 4063–4074. https://doi.org/10.1007/s11269-017-1728-0.

Georges, V., Fanny, Q., Phan, T.S.H., Tran, N.T.D., Nguyen, T., Luu, X.L., Nguyen, A.T., Nicolas, G., 2019. Flood-related risks in Ho Chi Minh City and ways of mitigation. J. Hydrol. 573, 1021–1027. https://doi.org/10.1016/j.jhydrol.2018.02.044.

Graham, W.J., 1999. A procedure for estimating loss of life caused by dam failure. U.S. Bureau of Reclamation, Dam Safety Office, Denver, USA, Report No. DSO-99-06. 44.

Ge, W., Jiao, Y., Sun, H., Li, Z., Zhang, H., Zheng, Y., Guo, X., Zhang, Z., Van Gelder, P., 2019. A method for fast evaluation of potential consequences of dam breach. Water 11 (11), 2224. https://doi.org/10.3390/w11112224.

Ge, W., Wang, X., Li, Z., Zhang, H., Guo, X., Wang, T., Gao, W., Lin, C., Van Gelder, P., 2021. Interval analysis of loss of life caused by dam failure. J. Water Res. Plan. Man. 147 (1), 04020098. https://doi.org/10.1061/(ASCE)WR.1943-5452.0001311.

Huang, D., Yu, Z., Li, Y., Han, D., Zhao, L., Chu, Q., 2017. Calculation method and application of loss of life caused by dam break in China. Nat. Hazards 85 (1), 39–57. https://doi.org/10.1007/s11069-016-2557-9.

Johnstone, W., Garrett, M., 2014. Return to Malpasset: Using the Life Safety Model to assess the effectiveness of community evacuation plans, ASDSO Annual Conference, 21-24 September, San Diego, USA.

Jonkman, S.N., Vrijling, J.K., Vrouwenvelder, A.C.W.M., 2008. Methods for the estimation of loss of life due to floods: a literature review and a proposal for a new method. Nat. Hazards 46 (3), 353–389. https://doi.org/10.1007/s11069-008-9227-5.

Kim, Y., Lee, M.J., 2020. Rapid change detection of flood affected area after collapse of the Laos Xe-Pian Xe-Namnoy Dam using Sentinel-1 GRD data. Remote Sens-Basel. 12 (12), 1978. https://doi.org/10.3390/rs12121978.

Kuller, K., Schoenholzer, K., Lienert, j.,, 2021. Creating effective flood warnings: a framework from a critical review. J. Hydrol. 602, 126708 https://doi.org/10.1016/j.jhydrol.2021.126708.

Latrubesse, E.M., Arima, E.Y., Dunne, T., Park, E., Baker, V.R., d'Horta, F.M., Wight, C., Wittmann, F., Zuanon, J., Baker, P.A., Ribas, C.C., Norgaard, R.B., Filizola, N., Ansar, A., Flyvbjerg, B., Stevaux, J.C., 2017. Damming the rivers of the amazon basin. Nature 546 (7658), 363–369.

Li, Z., Wang, T., Ge, W., Wei, D., Li, H., 2019a. Risk analysis of earth-rock dam breach based on dynamic Bayesian network. Water. 11 (11), 2305. https://doi.org/10.3390/w11112305.

Lumbroso, D.M., Sakamoto, D., Johnstone, W.M., Tagg, A.F., Lence, B.J., 2011. The development of a life safety model to estimate the risk posed to people by dam failures and floods. Dams Reservoirs J. 21 (1), 31–43.

Lumbroso, D., Davison, M., Body, R., Petkovšek, G., 2021. Modelling the Brumadinho tailings dam failure, the subsequent loss of life and how it could have been reduced. Nat. Hazard. Earth. Sys. 21 (1), 21–37.

Li, Z., Li, W., Ge, W., 2018. Weight analysis of influencing factors of dam break risk consequences. Nat. Hazards. Earth Sys. 18 (12), 3355–3362. https://doi.org/10.5194/nhess-18-3355-2018.

Li, W., Li, Z., Ge, W., Wu, S., 2019b. Risk evaluation model of life loss caused by dam-break flood and its application. Water. 11 (7), 1359. https://doi.org/10.3390/w11071359.

Lee, K.H., 2019. Simulation of dam-breach outflow hydrographs using water level variations. Water Resour. Manag. 33 (11), 3781–3797. https://doi.org/10.1007/BF02841991.

Pathak, S., Liu, M., Jato-Espino, D., Zevenbergen, C., 2020. Social, economic and environmental assessment of urban sub-catchment flood risks using a multi-criteria approach: a case study in Mumbai City. India. J. Hydrol. 591, 125216.

Peng, M., Zhang, L., 2012a. Analysis of human risks due to dam-break floods-part 1: a new model based on Bayesian networks. Nat. Hazards 64 (1), 903–933. https://doi.org/10.1007/s11069-012-0275-5.

Peng, M., Zhang, L., 2012b. Analysis of human risks due to dam-break floods-part 2: application to Tangjiashan landslide dam failure. Nat. Hazards 64 (2), 1899–1923. https://doi.org/10.1007/s11069-012-0336-9.

Penning-Rowsell, E., Floyd, P., Ramsbottom, D., Surendran, S., 2005. Estimating injury and loss of life in floods: a deterministic framework. Nat. Hazards 36 (1–2), 43–64. https://doi.org/10.1007/s11069-004-4538-7.

Peter, S.J., Siviglia, A., Nagel, J., Marelli, S., Boes, R.M., Vetsch, D., Sudret, B., 2018. Development of probabilistic dam breach model using Bayesian inference. Water Resour. Res. 54 (7), 4376–4400. https://doi.org/10.1029/2017WR021176.

Qi, H., Altinakar, M.S., 2012. GIS-Based decision support system for dam break flood management under uncertainty with two-dimensional numerical simulations. J. Water Res. Plan. Man. 140 (2), 194–200. https://doi.org/10.1061/(ASCE)WR.1943-5452.0000192.

RESCDAM. 2000. The use of physical models in dam-break flood analysis: rescue actions based on dam-break flood analysis. Final report of Helsinki University of Technology; Helsinki University of Technology: Helsinki, Finland. 57.

Sun, R., Wang, X., Zhou, Z., Ao, X., Sun, X., Song, M., 2014. Study of the comprehensive risk analysis of dam-break flooding based on the numerical simulation of flood routing. Part I: model development. Nat. Hazards 73 (3), 1547–1568. https://doi.org/10.1007/s11069-014-1154-z.

Thrysøe, C., Balstrøm, T., Borup, M., Löwe, R., Jamali, B., Arnbjerg-Nielsen, K., 2021. FloodStroem: a fast dynamic GIS-based urban flood and damage model. J. Hydrol. 600, 126521 https://doi.org/10.1016/j.jhydrol.2021.126521.

U.S. Department of the Interior, Bureau of Reclamation, 2015. RCEM - Reclamation consequence estimating methodology - interim - guidelines for estimating life loss for dam safety risk analysis.

Urbanik, T., 2000. Evacuation time estimates for nuclear power plants. J. Hazard. Mater. 75 (2), 165–180. https://doi.org/10.1016/S0304-3894(00)00178-3.

United States Army Corps of Engineers (USACE), 2016. HEC-RAS, river analysis system -hydraulic reference manual (version 5.0). Hydrologic Engineering Centre, Davis, California.

Wu, M., Wu, Z., Ge, W., Wang, H., Shen, Y., Jiang, M., 2021. Identification of sensitivity indicators of urban rainstorm flood disasters: a case study in China. J. Hydrol. 599, 126393 https://doi.org/10.1016/j.jhydrol.2021.126393.

Walder, J.S., Iverson, R.M., Godt, J.W., Logan, M., Solovitz, S.A., 2015. Controls on the breach geometry and flood hydrograph during overtopping of noncohesive earthen dams. Water Resour. Re. 51 (8), 6701–6724. https://doi.org/10.1002/2014WR016620.

Wang, B., Chen, Y., Wu, C., Peng, Y., Song, J., Liu, W., Xin, L., 2018. Empirical and semi-analytical models for predicting peak outflows caused by embankment dam failures. J. Hydrol. 562, 692–702. https://doi.org/10.1016/j.jhydrol.2018.05.049.

Wang, Z., Song, W., 2014. Study of estimation model of loss of life caused by dam break. J. Hohai Univ. (Natural Sci.) 42 (3), 205–210. https://doi.org/10.3876/j.issn.1000-1980.2014.03.004.

Xinhuanet, 2020. 56 people injured by dam break of a reservoir in Uzbekistan. http://www.xinhuanet.com/world/2020-05/02/c_1125936325.htm.

Xue, J., Wu, C., Chen, Z., Van Gelder, P.H.A.J.M., Yan, X., 2019. Modeling human-like decision-making for inbound smart ships based on fuzzy decision trees. Expert Syst. Appl. 115, 172–188.

Yang, Y., Guo, H., Wang, D., Ke, X., Li, S., Huang, S.R., 2021. Flood vulnerability and resilience assessment in China based on super-efficiency DEA and SBM-DEA methods. J. Hydrol. 600, 126470 https://doi.org/10.1016/j.jhydrol.2021.126470.

Yu, J., Wen, J., 2016. Multi-criteria satisfaction assessment of the spatial distribution of urban emergency shelters based on high-precision population estimation. Int. J. Disast. Risk Sc. 7 (4), 413–429. https://doi.org/10.1007/s13753-016-0111-8.

Zeng, Z., Guan, D., Steenge, A.E., Xia, Y., Mendoza-Tinoco, D., 2019. Flood footprint assessment: a new approach for flood-induced indirect economic impact measurement and post-flood recovery. J. Hydrol. 579, 124204 https://doi.org/10.1016/j.jhydrol.2019.124204.

Zhou, K., Li, L., Sheng, J., 2007. Evaluation model of loss of life due to dam breach in China. J. Safety Environ. 7 (3), 145–149. https://doi.org/10.3969/j.issn.1009-6094.2007.03.037.

Zhao, G., Bates, P.D., Neal, J., 2020. The impact of dams on design floods in the conterminous US. Water Resour. Res. 56 (3) https://doi.org/10.1029/2019WR025380.